Sensors and Materials, Vol. 27, No. 10 (2015) 993–1001
MYU Tokyo

S & M 1136

Enhanced Photocatalytic Activity of TiO_2–CNT Composites for Photoreduction of CO_2

Kim-Yang Lee[1,2], Abdul Rahman Mohamed[1,*] and Kazunori Sato[2,**]

[1]School of Chemical Engineering, Universiti Sains Malaysia, Penang, Malaysia
[2]Department of Environmental Engineering, Nagaoka University of Technology, Nagaoka, Japan

(Received February 16, 2015; accepted May 26, 2015)

Key words: photocatalysis, photocatalytic reduction of CO_2, TiO_2–CNT composite, titanium dioxide

In this work, we present a facile and dopant-free approach using a peroxo-titanium complex as a precursor to synthesize TiO_2–carbon nanotube (CNT) composites at various CNT loadings, ranging from 0 to 10 wt% (gram CNT per unit gram of TiO_2). The photocatalytic activity of as-synthesized composites on CO_2 reduction was studied. The as-synthesized composites were characterized by X-ray diffraction (XRD) and UV–visible spectroscopy. XRD analysis revealed that the as-produced TiO_2 was a mixture of anatase and rutile phase TiO_2. UV–vis spectra showed that the absorption edge of the as-synthesized composites was redshifted and exhibited an improvement in light absorbance as compared with the commercially available anatase TiO_2. Among the synthesized TiO_2–CNT composites, TiO_2–CNT with 5 wt% CNT loading showed the highest photocatalytic activity on CO_2 reduction. A possible reaction mechanism for the photoreduction of CO_2 was proposed.

1. Introduction

The increasing demand for energy supplies has accelerated the depletion of fossil fuels, and sooner or later, humankind will face a shortage of fossil fuels. At the same time, the combustion of fossil resources, including petroleum and natural gas, is always coupled with the emission of greenhouse gases, particularly carbon dioxide (CO_2), which is regarded as the primary greenhouse gas. The emergence of clean, sustainable energy technology is vital, which not only prevents the risk of running out of conventional fossil fuels, but at the same time mitigates global warming by reducing CO_2 emissions. Solar energy is the most abundantly available renewable energy, and the photocatalytic conversion of CO_2 to solar fuels is therefore viewed as a plausible solution to simultaneously mitigate atmospheric CO_2 and to achieve sustainable energy generation.[1,2]

*Corresponding author: e-mail: chrahman@eng.usm.my
**Corresponding author: e-mail: sato@analysis.nagaokaut.ac.jp

ISSN 0914-4935

Since the first demonstration of the photocatalytic reduction of CO_2 in aqueous suspensions of different semiconductor powders to form organic compounds by Inoue *et al*.,[3] the photoreduction of CO_2 to solar fuels has become an area of active research. Over the past decades, significant work has been carried out to develop effective photocatalysts for CO_2 reduction. Many types of semiconductor photocatalysts, such as TiO_2,[4,5] ZnO,[6] ZrO_2,[7] $BiVO_4$,[8,9] and combinations thereof, have been widely studied for this purpose. Among these semiconductor photocatalysts, TiO_2 is by far the most studied, owing to its nontoxicity, long-term stability, low cost, and environmentally benign properties.[10] However, the practical uses of TiO_2 in the photocatalytic reduction of CO_2 are still hindered by its large band gap (3.2 eV) and ineffective utilization of visible light, resulting in low quantum efficiency in photocatalytic reactions.[11] In this regard, various strategies have been employed to improve its photocatalytic behaviour, including textural design, doping, and coupling with compounds that are photoactive in the visible region.[12]

In recent years, the employment of carbon nanomaterials for photocatalysis enhancement is among one of the measures attempted, owing to the materials' unique properties and electron transfer ability. In this work, a facile method for the synthesis of TiO_2–carbon nanotube (CNT) composites using a peroxo-titanium complex as a TiO_2 precursor has been developed. The effect of different CNT loadings on photocatalytic activity for the reduction of CO_2 has been studied as well.

2. Materials and Methods

2.1 *Chemicals*

All chemicals were reagent-grade, and distilled water was used throughout the experiments. Titanium tetra-*n*-butoxide [$Ti(O\text{-}n\text{-}C_4H_9)_4$, Soekawa Chemicals, >99% purity] was used as the titania precursor. Hydrogen peroxide (H_2O_2, 30%), sulfuric acid (H_2SO_4, 97%), and nitric acid (HNO_3, 70%) were purchased from Nacalai Tesque, Japan. Pure anatase titania nanopowder (TiO_2, Soekawa Chemicals, >99.9% purity) was used as a photocatalyst control. All chemicals were used as received without any further purification. CNTs used in the experiments were multi-walled CNT produced from the catalytic decomposition of methane,[13] which contains both metallic and semiconductor nanotubes. The CNT was treated with acid by the continuous stirring of 1 g of CNT in a mixture of HNO_3 and H_2SO_4 in a volume ratio of 1:3 and a concentration of 5 M and was then heated at 90 °C for 3 h. The mixture was then filtered and repeatedly washed with distilled water until pH 7 was achieved. The acid-treated CNT was dried overnight and was then ready for use. The same batch of acid-treated CNT was used throughout the experiments to ensure the homogeneity of CNT in the as-produced TiO_2–CNT composites.

2.2 *Synthesis of TiO_2 and TiO_2–CNT composites*

In the synthesis of photocatalysts, a specific amount of acid-treated CNT was dispersed in 200 ml of distilled water to achieve a specific mass ratio of CNT to TiO_2 (0, 1, 5, and 10 wt%); the samples were labelled as T0C, T1C, T5C, and T10C, respectively. The CNT suspension was sonicated for 30 min, then 5 ml of titanium tetra-*n*-butoxide was

added, which resulted in the immediate precipitation of titanium hydrates. After filtration and washing with distilled water, 80 ml of H_2O_2 was added dropwise to the precipitate to form a peroxo-titanium intermediate.[14] The solution was stirred at 60 °C until a gel formed and was dried in an air oven overnight. The resulting solid material was calcined at 350 °C for 5 h.

2.3 *Characterization*

UV–visible absorbance spectra were obtained using a UV–visible spectrophotometer (Jasco, V-7200) at room temperature in the wavelength ranging from 200–800 nm. A fixed amount of the sample was placed into the powder sample holder and spread uniformly. Phase identification was made with an X-ray diffractometer (Rigaku RAD-3A) operating at 40 kV and 30 mA using monochromated Cu-Kα radiation at a scan rate (2θ) of 0.02° s^{-1}.

2.4 *Photocatalytic reduction of CO_2*

The photocatalytic reduction of CO_2 in water was carried out in a one-sided quartz photocell under irradiation by a spot light source (Hamamatsu LC8, 200 W Hg–Xe lamp with λ_{max} = 365 nm) for 3 h. In each experimental run, 50 mg of photocatalyst was dispersed in the photocell, which contained 25 ml of distilled water. The solution was bubbled with CO_2 for 30 min to reach saturation prior to light irradiation. The gas products were collected and analyzed at 1 h intervals with a higly sensitive gas chromatograph (Shimadzu's Tracera GC-2010 Plus) equipped with a barrier discharge ionization detector (BID) to determine the components and to investigate the catalytic activity. A series of repeated runs was conducted to verify the accuracy of measurements, and the average relative areas of the product peaks are reported in this article. Three control experiments were conducted to ensure that any product formed was due to the photoreduction of CO_2, namely, (i) under dark conditions (without irradiation by the light source), (ii) blank test without photocatalyst, and (iii) CO_2-free test, i.e., solution purge with argon gas prior to irradiation to remove dissolved CO_2.

3. Results and Discussion

3.1 *Characterization of TiO_2–CNT composites*

Figure 1 shows the X-ray diffraction (XRD) patterns of TiO_2–CNT composites synthesized with different CNT contents as compared with those of the acid-treated CNT and pure anatase TiO_2. There are no apparent peaks for CNT, as CNT has a low atomic number and thus cannot be resolved by XRD.[15] As shown in the XRD patterns, the TiO_2–CNT composites (spectra c–f) were found to process diffraction patterns similarly to the as-prepared TiO_2 without CNT loading (namely, T0C, spectra b), indicating that the CNT loading did not alter the crystal phase of TiO_2 crystallites.

The XRD patterns of TiO_2–CNT composites further confirmed a mixture of anatase and rutile phase TiO_2. The reflection peaks of 110 (2θ = 27.4°), 101 (2θ = 36.1°), and 111 (2θ = 41.3°) clearly represent the formation of rutile TiO_2 (JCPDS#21-1276). The formation of the rutile phase is unexpected, as the phase transformation from anatase to rutile

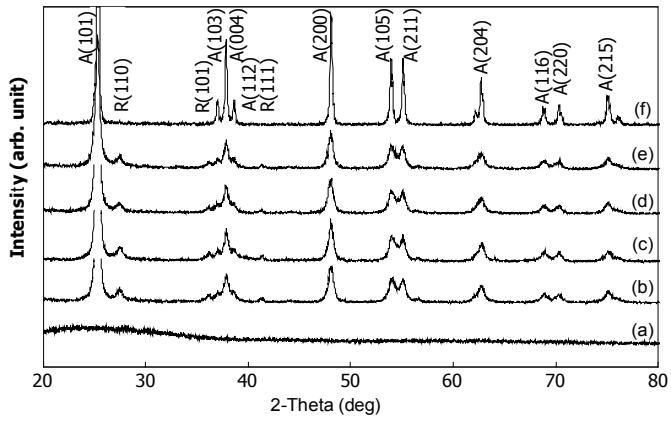

Fig. 1. XRD patterns of (a) CNT, (b) T0C, (c) T1C, (d) T5C, (e) T10C, and (f) anatase TiO_2.

usually occurs upon high-temperature calcinations (typically above 600 °C) of TiO_2.[16] This transformation could be attributed to the presence of oxygen defects formed in the peroxo-titanium complex,[17] in which the Ti atoms are bridged by two peroxy groups to form an octahedron. The decomposition of the peroxo groups led to the formation of small rutile chains. These chains were closely packed, interacted with each other, and finally arranged into the rutile structure.[18,19] The crystallite size of TiO_2 was calculated using Scherrer's equation based on the most intense reflection peak at 101.[20] The TiO_2 crystallite sizes for anatase TiO_2, T0C, T1C, T5C, and T10C were 41.4, 16.9, 16.1, 15.8, and 17.0 nm, respectively. The amount of rutile phase in the as-produced TiO_2–CNT composites was calculated using Spurr's equation.[21] The corresponding rutile phase amounts for T0C, T1C, T5C, and T10C were 8.44, 9.47, 6.91, and 7.41%, respectively.

The light absorption profiles of the as-prepared TiO_2–CNT composites, together with the pure anatase TiO_2 and acid-treated CNT, were measured by UV–vis diffuse reflectance spectroscopy. As illustrated in Fig. 2(a), the pure anatase and all the TiO_2–CNT composites displayed typical absorptions with an intense transition in the UV region, which is attributed to the intrinsic band gap absorption of TiO_2 due to the electron transitions from the valence band to the conduction band ($O_{2p} \rightarrow Ti_{3d}$).[22] It is worth mentioning that the pure anatase TiO_2 shows trace absorption above its fundamental absorption edge (approximately 400 nm), whereas the fundamental absorption edge of TiO_2 synthesized from the peroxotitanium complex as a precursor (sample T0C, with 0 wt% CNT content) was redshifted to ~430 nm, suggesting a narrowing of the band gap. This was confirmed by a Tauc plot of the modified Kubelka–Munk function with linear extrapolation, as shown in Fig. 2(b). The approximate band gap of T0C was 3.07 eV. The redshifted behaviour could be assigned to the variation in the lattice parameter from oxygen excess defects in accordance with other reports.[19,21] The same redshifted behaviour was observed in all the TiO_2–CNT composites, for example, the fundamental absorption edge for T1C and T5C is ~420 nm. The band gaps of T1C and T5C were approximately 3.08 and 3.14 eV, respectively. However, the band gap of T10C could

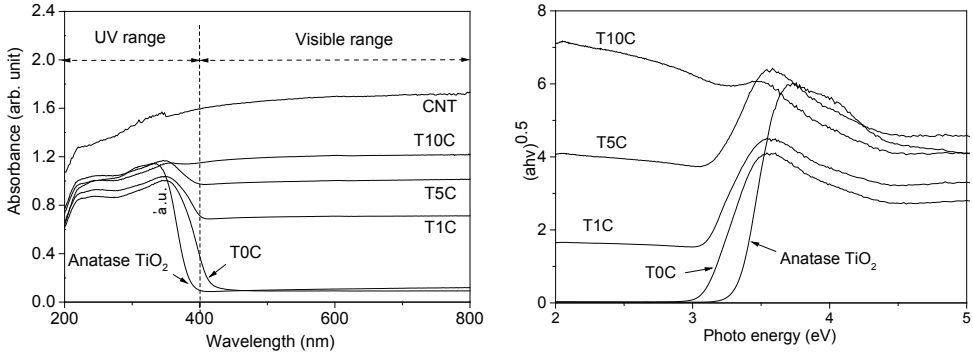

(a) (b)

Fig. 2. (a) UV–vis diffuse reflection spectra and (b) corresponding Tauc plots of anatase TiO_2 and as-produced composites.

not be determined from the Tauc plot. Furthermore, it can clearly be seen that the TiO_2–CNT composites exhibited an increasing absorption in the visible range (>400 nm) with increasing CNT content [Fig. 2(a)]. Such a trend is in agreement with the composite's color changing from white to dark grey. An increase in light absorption is favorable as light absorption is one of the critical factors for a photocalayst.

3.2 *Evaluation of CO_2 photoreduction*

The photocatalytic reduction of CO_2 with water over the as-prepared TiO_2–CNT composites was carried out at room temperature and atmospheric pressure. Control experiments were also performed under three conditions: (1) without light irradiation, (2) blank test (without photocatalyst), and (3) solution purge with argon gas prior to irradiation to remove dissolved CO_2. In both control runs (1) and (2), no appreciable CO nor CH_4 gas was detected. Meanwhile, a trace amount of hydrogen was detected in control run (3), which was attributed to the splitting of water. These control runs confirmed that any product yield was from the photocatalytic reduction of CO_2, and that a light source was essential for the process.

Figure 3 shows the yield of gaseous products from CO_2 photoreduction over pure anatase TiO_2 and as-produced composites. The evaluation of the photocatalytic reduction of CO_2 demonstrated that the pure anatase TiO_2 showed no appreciable CO nor CH_4 gas peak after 3 h of light irradiation. Among all the studied TiO_2–CNT composites, T0C and T1C exhibited the lowest efficiency for CO_2 reduction. Only a trace amount of CO was detected for either photocatalyst. As discussed earlier, the as-produced T0C is a mixture of anatase and rutile TiO_2. The enhanced photocatalytic activity of T0C compared with that of the pure anatase could be attributed to the synergetic effect of anatase–rutile phase junction. It is because the anatase–rutile phase junction is capable of inhibiting the recombination of electron–hole pairs, by allowing the photoinduced electrons to transfer from the conduction band of rutile to the conduction band of anatase.[23] Furthermore, the band alignment of anatase–rutile TiO_2 lowers the effective band gap,

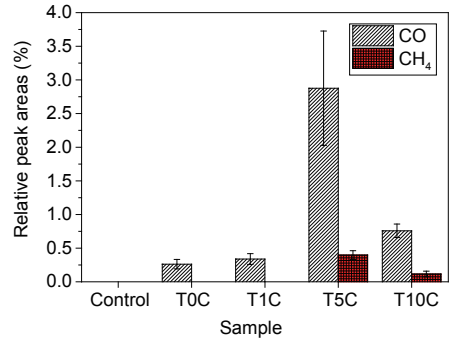

Fig. 3. (Color online) Yield of CO and CH_4 produced over all samples.

which is confirmed by a UV–vis study. Such band alignment has facilitated the electron–hole separation, hence the T0C exhibited higher photocatalytic activity than the control pure-phase anatase TiO_2.

Meanwhile, photocatalyst T5C exhibited the highest photocatalytic activity in terms of CO production, together with a trace amount of CH_4 detected. With a further increase in CNT loading to 10 wt% (sample T10C), both CO and CH_4 were detected, but the yields of both products were decreased. The decrease in photocatalytic activity as compared with that of the T5C photocatalyst could be due to a higher loading of CNT, which may shield the TiO_2 from absorbing UV light.[15] As for the formation of CH_4, the CB flatband potential of TiO_2 ($E^o = -0.5$ V) is more negative than the reduction potential of CO_2/CH_4 ($E^o = -0.24$ V);[19] therefore, the reaction is thermodymanically stable. However, the most challenging aspect is that the reaction requires eight electrons to reduce CO_2 to CH_4. This is the reason why the yield of CH_4 is much lower than that of CO. It is worth mentioning that the formation of CH_4 is thermodynamically more feasible than the formation of CO if the quantities of excited protons and electrons are sufficient. Therefore, an increase in the excited electron density would encourage the formation of CH_4. It has been suggested that CNT plays the role of an electron sink[24] and an electron-transfer channel.[15] When a light source irradiated TiO_2–CNT composites, the excited electons transfer from TiO_2 particles to CNT via the TiO_2–CNT heterojunction. The transfer of electrons to CNT would reduce the trapping of electrons in the lattice of TiO_2, subsequently prolonging the lifetime of electron–hole pairs.[24] During the photoreduction process, water undergoes oxidation by photoinduced holes, generating oxygen and H^+ ions, and CO_2 is reduced to CO or CH_4 by 2 or 8 electrons, respectively. As the lifetime of electron–hole pairs is extended and the electrons move freely along the CNT, the photocatalyst becomes more reactive.[15] Furthermore, the role of CNT as an electron sink enhances the denseness of excited electrons, and thus favors the formation of CH_4. This could be the reason why CH_4 was only detected over T5C and T10C. It is worth mentioning that hydrogen (H_2) was not detected by the GC. This could be attributed to the photogenerated H^+ ions and $H\cdot$ radicals being rapidly consumed by CO_2 during the process. Similar outcomes have been reported elsewhere[25,26] during the photocatalytic reduction of CO_2 with water using TiO_2-based photocatalysts.

3.3 *Possible reaction mechanism*

The photoreduction of CO_2 is a redox reaction involving the oxidation of water by holes (h^+) and the reduction of CO_2 by photoexcited electrons (e^-). Upon irradiation, electrons were excited to the conduction band (e^-_{cb}) of TiO_2, leaving positively charged holes in the valence band (h^+_{vb}), which resulted in electron–hole separation [eq. (1)]. The generated electrons and holes subsequently initiated the CO_2 photoreduction process by reacting with CO_2 and water. The positively charged holes oxidized the absorbed water, generating H^+ ions and oxygen [eq. (2)]. On the other hand, CO_2 was reduced by the photoexcited electrons to CO and CH_4, for which 2 and 8 electrons were required, respectively [eqs. (3) and (4)]. The overall reaction path for the formation of CO and CH_4 over the as-synthesized composites in this study is summarized in eqs. (5) and (6).

$$TiO_2 \rightarrow TiO_2\,(e^-_{cb}) + TiO_2\,(h^+_{vb}) \quad (1)$$

$$TiO_2\,(2h^+_{vb}) + H_2O \rightarrow TiO_2 + 2H^+ + \tfrac{1}{2}O_2 \quad (2)$$

$$TiO_2\,(2e^-_{cb}) + CO_2 + 2H^+ \rightarrow TiO_2 + CO + H_2O \quad (3)$$

$$TiO_2\,(8e^-_{cb}) + CO_2 + 8H^+ \rightarrow TiO_2 + CH_4 + 2H_2O \quad (4)$$

$$CO_2 + 2H^+ + 2e^- \rightarrow CO + H_2O \quad (5)$$

$$CO_2 + 8H^+ + 8e^- \rightarrow CH_4 + 2H_2O \quad (6)$$

A schematic of the enhanced electron transfer and reactant transformation using TiO_2–CNT composites for CO_2 photoreduction is shown in Fig. 4. Upon light irradiation,

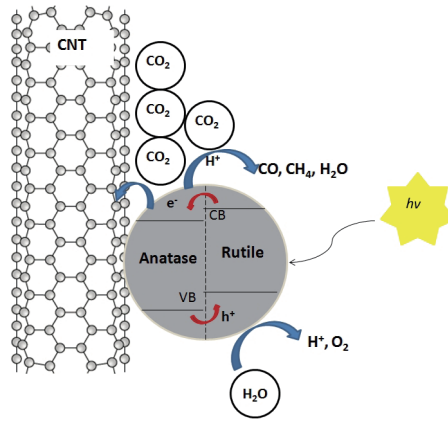

Fig. 4. (Color online) Proposed schematic of electron transfer and reactant transformation using TiO_2–CNT composites.

TiO_2 underwent charge separation, generating electron–hole pairs. Normally, these electron–hole pairs recombine quickly and only a fraction of the electrons and pairs are consumed in the photocatalytic reaction. Such rapid recombination rate of electron–hole pairs leads to low photocatalytic activity.[15] With the presence of CNT in the composites, the photoexcited electrons are transported to the neigboring CNT, prolonging the lifetime of electron–hole pairs, and thus enhancing the photocatalytic activity for CO_2 reduction. Furthermore, CNT plays the role of an electron sink, which enhances the density of photoexcited electrons and encourages the formation of CH_4.

4. Conclusion

TiO_2–CNT composites with an enhanced photocatalytic activity were synthesized via a facile method using a peroxotitanium complex as a percursor. The as-produced TiO_2–CNT composites consist of a mixture of anatase–rutile phase TiO_2, and exhibited an enhanced photocatalytic activity compared with the pure anatase TiO_2. The absorption edge of as-synthesized composites was redshifted and exhibited an improvement in light absorbance. An increase in CNT content led to a significant increase in light absorption in the visible range (>400 nm). Among the composites synthesized, the composite with 5 wt% loading of CNT demonstrated the best performance for the photocatalytic reduction of CO_2. A further increase in CNT content decreased the yield of CO and CH_4, which may due to the high content of CNT to shield the TiO_2 from absorbing UV light.

Acknowledgements

The authors acknowledge the Minister of Higher Education of Malaysia (LRGS: 203/PKT/6723001), Universiti Sains Malaysia (IReC: 1002/PJKIMIA/910404), and Nagaoka University of Technology (Pacific Rim Project) for the financial support.

References

1 Y. Izumi: Coord. Chem. Rev. **257** (2012) 171.
2 G. Centi and S. Perathoner: ChemSusChem. **3** (2010) 195.
3 T. Inoue, A. Fujishima, S. Konishi and K. Honda: Nature **277** (1979) 637.
4 K. Kočí, L. Obalová, L. Matějová, D. Plachá, Z. Lacný, J. Jirkovský and O. Šolcová: Appl. Catal. B Environ. **89** (2009) 494.
5 Q. D. Truong, T. H. Le, J. Y. Liu, C. C. Chung and Y. C. Ling: Appl. Catal. A Gen. **437–438** (2012) 28.
6 O. K. Varghese, M. Paulose, T. J. LaTempa and C. A. Grimes: Nano Lett. **9** (2009) 731.
7 Y. Kohno, T. Tanaka, T. Funabiki and S. Yoshida: Phys. Chem. Chem. Phys. **2** (2000) 2635.
8 J. Mao, T. Peng, X. Zhang, K. Li and L. Zan, Catal. Commun. **28** (2012) 38.
9 Y. Liu, B. Huang, Y. Dai, X. Zhang, X. Qin, M. Jiang and M. H. Whangbo: Catal. Commun. **11** (2009) 210.
10 A. Fujishima, X. Zhang and D. A. Tryk: Surf. Sci. Rep. **63** (2008) 515.
11 A. L. Linsebigler, G. Lu and J. T. Yates Jr.: Chem. Rev. **95** (1995) 735.
12 Q. Zhang, L. Liu and Y. Li: Energy Technology 2012: Carbon Dioxide Management and Other Technologies, eds. M. D. Salazar-Villalpando, N. R. Neelameggham, D. P. Guillen, S. Pati and G. K. Krumdick (Wiley, Hoboken, 2012) Chap. 1.

13 W. M. Yeoh, K. Y. Lee, S. P. Chai, K. T. Lee and A. R. Mohamed: Xinxing Tan Cailiao **24** (2009) 119.
14 C. D. Nordschow and A.R. Tammes: Anal. Chem. **40** (1968) 465.
15 J. Yu, T. Ma and S. Liu: Phys. Chem. Chem. Phys. **13** (2011) 3491.
16 D. A. H. Hanaor and C. C. Sorrell: J. Mater. Sci. **46** (2011) 855.
17 R. D. Shannon: J. Appl. Phys. **35** (1964) 3414.
18 Y. Zhang, L. Wu, Q. Zeng and J. Zhi: J. Phys. Chem. C **112** (2008) 16457.
19 L. L. Tan, W. J. Ong, S. P. Chai and A. R. Mohamed: Chem. Commun. **50** (2014) 6923.
20 J. I. Langford and A. J. C. Wilson: J. Appl. Crystallogr. **11** (1978) 102.
21 R. A. Spurr: Anal. Chem. **29** (1957) 760.
20 M. R. Hoffmann, S. T. Martin, W. Choi and D. W. Bahnemann: Chem. Rev. **95** (1995) 69.
21 V. Etacheri, M. K. Seery, S. J. Hinder and S. C. Pillai: Adv. Funct. Mater. **21** (2011) 3744.
22 W. J. Ong, L. L. Tan, S. P. Chai, S. T. Yong and A. R. Mohamed: Nanoscale **6** (2014) 1946.
23 D. O. Scanlon, C. W. Dunnill, J. Buckeridge, S. A. Shevlin, A. J. Logsdail, S. M. Woodley, C. R. A. Catlow, M. J. Powell, R. G. Palgrave, I. P. Parkin, G. W. Watson, T. W. Keal, P. Sherwood, A. Walsh and A. A. Sokol: Nat. Mater. **12** (2013) 798.
24 M. M. Gui, S. P. Chai, B. Q. Xu and A. R. Mohamed: Sol. Energy Mater. Sol. Cells **122** (2014) 183.
25 X. Li, Z. Zhuang, W. Li and H. Pan: Appl. Catal. A Gen. **429–430** (2012) 31.
26 W. J. Ong, L. L. Tan, S. P. Chai, S. T. Yong and A. R. Mohamed: Nano Res. **10** (2014) 1528.